Multiscale granular mechanics: A neutron diffraction based experimental approach

Athanasopoulos, Stefanos

2019

Document Version:
Publisher's PDF, also known as Version of record

Department of Construction Sciences
Solid Mechanics

ISRN LUTFD2/TFHF-19/1061-SE(1-132)
ISBN: 978-91-7895-259-5 (print)
ISBN: 978-91-7895-260-1 (pdf)

Multiscale granular mechanics: A neutron diffraction based experimental approach

Doctoral Thesis by

Stefanos D. Athanasopoulos

Printed by Media-Tryck AB, Lund, Sweden
For information, address:
Division of Solid Mechanics, Lund University, Box 118, SE-221 00 Lund, Sweden
Homepage: http://www.solid.lth.se

Στη μνήμη του πατέρα μου, Δημήτρη

Preface

This thesis is the result of my doctoral studies at the Division of Solid Mechanics of Lund University the past 6 years, since October 2013.

First of all, I would like to express my deepest gratitude to my supervisor, Steve. Putting in words what it means to me having him as the supervisor of my PhD is rather difficult. His continuous support and advice the past few months I spent trying to make this thesis a reality is only the last addition in a very long list of reasons why he has my highest appreciation, with the very first one being the fact that 6 years ago he offered me the opportunity to have the pleasure of working with him and, especially, learning by him.

It is a rare thing being motivated, even happy, every morning you wake up to go to work and the past 6 years I was lucky enough to have that. Not only because I loved what I did for my PhD, but, most importantly, because I enjoyed so much the time I spent with all the people of the "solid group", past and current, fellow PhD students and seniors! I thank all of them for this. Johan, Sara and Niklas, however, deserve a slightly bigger thanks, for all the fun times we also had out of the office and, more than that, because the three of them, together with all the rest of the friends I made the past 6 years, made Sweden my "home". A rather important role to that had my flat mate and very old friend, back from Greece, Rigos (a.k.a., Alexandros, or Alex), without whom, I am very certain that all the time I was spending at home working, which increased dramatically the past few months, would have been considerably more dull.

I would also like to thank all my friends back in Greece, or shall I say, back from Greece, as many of them are scattered around the globe. They were always "here" for me, even if they were hundreds, or even thousands, of kilometers away. In particular, I would like to individually thank Katerina, Stefanos and Kimon, my three oldest and best friends. I am pretty certain they know why...

Finally, I want thank my family, my two sisters and my brother, who never stopped caring for and supporting their little brother, each one of them with her/his own way, and of course my mother. Although I am certain that, being the kind of person she is, she does not need to see it written here, I am writing it anyway. Mom, thank you for being such a devoted parent and selfless person, in general. You have always supported me in all my endeavours, amongst which was the pursuit of my PhD.

Lund, September 2019
Stefanos D. Athanasopoulos

Abstract

Granular media (i.e., assemblies of grains, containing voids), such as sand, are highly complex materials, possessing inherently heterogeneous structure and properties that are manifested by the mobility and interaction of their constituent particles. Despite having been widely studied for centuries (i.e., the study of granular media in modern science essentially begins with the work of Charles-Augustin de Coulomb on sand, in 1776), there still exist key pieces of information regarding their (micro-)mechanical behaviour that have been largely eluding the scientific community. More specifically, under the effect of applied stress, these materials exhibit highly inhomogeneous mechanical behaviours, indicating varying and evolving local stress-strain relationships. As far as the strain is concerned, over the past decades, increasingly fine details have been revealed into the underlying grain-scale mechanisms, the origins of heterogeneous behaviour, including localisation, and how these lead to macroscopic material failure. However, details on the evolution of force/stress distribution are a key, missing piece of information and to be understood, requires appropriate, spatially-resolved local measurements.

This thesis presents a novel, multiscale experimental approach, to characterise quantitatively the (micro-)structural evolution of granular media during loading, by associating traditional macroscale boundary measurements with microscale information acquired by neutron diffraction (ND), as well as digital image correlation (DIC), at a mesoscale in between. The ND method provides mapping of the distribution of stresses throughout the granular skeleton of the material, by inference from measured crystallographic strains of the grains, whilst DIC provides the complementary total strain field mapping, opening the possibility for local stress-strain analysis. A key component that enabled this novel approach is the development of a new, specially designed plane-strain loading apparatus. A series of experiments was realised with this apparatus, demonstrating the potential of the experimental approach through combined stress and strain mapping. These experimental developments also highlighted the need for appropriate, reference ND measurements for granular media, for the effective employment of the ND method, which, as of yet, do not exist. This need has been addressed and a newly assembled dataset of reference measurements for the material under study (i.e., Fontainebleau quartz sand) is presented in this thesis. With this reference dataset, a proper basis has been set for the better analysis of future experiments. Together, these experimental developments and results have laid the foundation for future, more detailed investigations of granular mechanics, where both stress and strain may be characterised locally in a specimen under load, in a full-field sense.

List of appended papers

This doctoral thesis is based on the following manuscripts:

Paper A
Stefanos D. Athanasopoulos, Stephen A. Hall, Joe F. Kelleher, Thilo Pirling, Jonas Engqvist, and Johan Hektor
Mapping grain strains in sand under load using neutron diffraction scanning
In: Micro to MACRO Mathematical Modelling in Soil Mechanics. Trends in Mathematics (Giovine P., Mariano P., and Mortara G. (Eds.)), 2018, 23-33.

Paper B
Stefanos D. Athanasopoulos, Stephen A. Hall, and Joe F. Kelleher
A novel multiscale neutron diffraction based experimental approach for granular media
Géotechnique Letters (Ahead of print), 2019, 1-15

Paper C
Stefanos D. Athanasopoulos, Gary D. Couples, and Stephen A. Hall
A new apparatus for multiscale stress-strain measurements on granular media under plane-strain loading conditions
To be submitted for publication in Acta Geotechnica

Paper D
Stefanos D. Athanasopoulos, Stephen A. Hall, and Joe F. Kelleher
Determination of grain-orientation dependent granular stress in quartz sand by neutron diffraction
To be submitted for publication in Granular Matter

Own Contribution
The author of this thesis has taken the main responsibility for the preparation and writing of all appended papers. The apparatus presented in Paper C has been been developed in collaboration with the co-authors. The apparatus presented in Paper D has been been developed in collaboration with the 1st co-author. The experiments and analysis of the data in Papers A, B, and D were carried out by the author in collaboration with the co-authors.

Contents

Chapter 1

Introduction

> Pick up a single grain (of sand) from the beach, look at it through a magnifying glass, and you have embarked on a journey ...
>
> Michael Welland

Granular media, generally considered as assemblies of grains, containing voids, constitute an extremely vast family of materials and are ubiquitous in nature. Since Coulomb's fundamental work on the shear strength of soil in 1776[1], the earliest published study on granular media, this has become a wide and active research area, including contributions from numerous eminent scientists. These include the pioneering works of Michael Faraday on vibrating powders (1831), Henry Darcy on flows through porous media (1856), Osborne Reynolds describing the phenomenon of dilatancy (1885) and Karl Terzaghi on water-saturated granular geomaterials (1943).

Even though granular media have been so long and so extensively studied, there still exist key pieces of information regarding their (micro-)mechanical behaviour that have been largely eluding the scientific community. To this end, the main objective of this PhD thesis is to provide new insights into granular mechanics, by presenting a novel, multiscale experimental approach for the analysis of granular (geo-)materials.

This, introductory chapter, starts with a brief overview on granular media, focusing on certain fundamental characteristics. Subsequently, the latest advances of experimental (geo-)mechanics in the context of the topic of the current PhD project are shortly discussed and, finally, the chapter concludes with the scope and structure of this thesis.

[1] Coulomb first presented his work to the French Academy of Sciences in 1773, but his essay was not published until three years later, in 1776.

1.1 Granular media: A brief overview

Granular media are (single-phase) particulate materials and as such, they can be broadly defined as collections of discrete macroscopic particles interacting with each other through contact, rather than long range forces. They are inherently in a non-equilibrium state as their constituent particles are large enough to avoid rearrangement under thermal fluctuations (i.e., ordinary temperature plays no role) and also, when in contact, they are characterised by dissipative intergranular interactions, due to static friction and inelasticity of collisions (Jaeger et al., 1996; Papadopoulos et al., 2018).

Despite their seeming simplicity, they can exhibit characteristics of solids (e.g., create a static pile), liquids (e.g., flow out of a container), as well as gases (i.e., if strongly agitated, the contacts between the grains become highly infrequent and the material enters a gaseous state) and, in fact, these regimes may also coexist within a single configuration (Figure 1.1). To this end, Jaeger, Nagel and Behringer (1996) claimed that since granular media behave differently from any other classical state of matter (i.e., solid, liquid and gas), they should be considered as an additional state.

The focus of the present PhD project is on one of the most widely studied types of geomaterials, sand, in its solid state. Sand can be created in different ways and can be composed of a wide variety of substances, but the most common process is weathering and the majority of earth's sand grains are made of quartz (Welland, 2009). Quartz sand consists of the most common form of silica (silicon dioxide – SiO_2), its stable polymorph at ambient conditions, α-quartz (for more information, see Paper D). The sand studied herein is the NE34 Fontainebleau quartz sand, a high quartz purity sand (i.e., 99.7 % quartz) with an average grain size, D_{50}, of 210 µm.

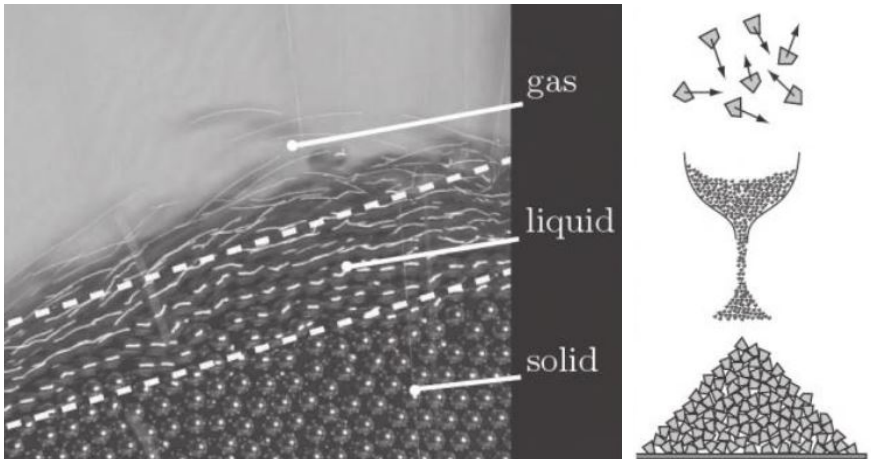

Figure 1.1: Coexistence of solid, liquid and gaseous regimes within a single configuration of a granular medium (Andreotti et al., 2013).

1.2 Advances in experimental mechanics for granular (geo-)materials

As the now considered "father" of soil mechanics, Karl Terzaghi, once said: *"Unfortunately, soils are made by nature and not by man, and the products of nature are always complex"* (Goodman, 1999). In the present case, the complex products of nature are granular geomaterials, such as sand, possessing inherently heterogeneous structure and properties that are manifested by the mobility and interaction of their constituent particles. As a result, under the effect of applied stress, these materials exhibit highly inhomogeneous behaviours and mechanics, which might vary significantly throughout their granular skeleton, indicating varying and evolving local stress-strain relationships. Understanding and characterising such relationships has always been central in the study of (geo-)mechanics and, over the past 40 years or so, strain localisation phenomena have been extensively investigated (e.g., Desrues et al., 2018).

The role of full-field measurement methods (i.e., methods that provide a field record of a quantity, rather than point-wise data) in the study of localised phenomena and the (micro-)mechanisms leading to macroscopic material failure has been of paramount importance in (geo-)mechanics. Viggiani and Hall (2008) presented an overview of different, at the time, cutting-edge full-field techniques, including digital image correlation (DIC), ultrasonic tomography and X-ray tomography, as well as examples of their application in experimental geomechanics (see references therein). However, as Viggiani and Hall stated, full-field measurement is a rapidly growing subject in experimental mechanics, in general, and this becomes evident in the continuous improvement of already existing techniques and by the emergence of new ones.

For many decades, large-scale research facilities, such as synchrotron light sources and neutron radiation sources[2] have been a particularly important battleground for scientists, to expand the frontiers of knowledge in a wide range of research disciplines, most notably in material science.

Regarding granular (geo-)materials and the investigation of their mechanics, in-situ studies have taken place at such facilities for more than a decade, as, for instance, the examples reported by Viggiani and Hall (2008) of in-situ X-ray tomography experiments realised at a synchrotron. Since then, the number of such applications for granular (geo-) materials has grown significantly. In more recent years, there has also been an increasing number of studies employing neutron tomography. However, even if, through the employment of these two advanced experimental techniques it has become possible to reveal intricate details on strain localisation phenomena in such materials (e.g., Hall et al., 2010), details on the distribution and evolution of stresses are, generally, still missing.

Stress distribution throughout granular media and its evolution with loading is directly associated with the existence of force chains (e.g., Santamarina, 2003; Peters et al.,

[2]Synchrotrons are, essentially, extremely powerful X-ray sources, but this type of large-scale facility is outside the scope of this thesis and will not be discussed any further. As for neutron sources, they are discussed in Chapter 2.

2005). From an experimental perspective, the concept of force chains has been studied for over half a century now, mainly by the technique of photoelasticity (Figure 1.2), both on two-dimensional (2D) analogues of granular media (e.g., Drescher and De Jong, 1972; Majmudar and Behringer, 2005) and three-dimensional (3D) materials (e.g., Allersma, 1982; Muir Wood and Lesniewska, 2011), and, lately, by other techniques as well, such as X-ray tomography (e.g., Oda et al., 2004; Saadatfar et al., 2012) and confocal microscopy (e.g., Brujić et al., 2003; Zhou et al., 2006). However, apart from very few exceptions (e.g., Oda et al., 2004), these experimental works involved synthetic materials.

In the attempt to study the evolution of force/stress distribution in natural granular media, such as sand, two scattering based methods have recently been employed, which are available at large-scale facilities. These are 3D X-ray diffraction (3DXRD) and neutron diffraction (ND). As discussed in more detail in the following chapter for ND, the principle to deduce stresses through these methods, which is the same for both, relies on the fact that the constituent grains of a granular specimen under load may serve as intrinsic strain gauges. From the measurements provided by these, "grain strain gauges", at first the elastic component of the crystallographic – or grain – strains can be derived and, consequently, directly by making use of Hooke's law, grain-scale stresses can be deduced. In the case of 3DXRD the acquired measurements are for each grain individually (e.g., Hall et al., 2011; Hall and Wright, 2015; Hurley et al., 2016; Hurley et al., 2017), whilst for ND they are averaged values over small sub-volumes of the specimen (e.g., Hall et al., 2011; Wensrich et al., 2012; Zhang et al., 2016; Athanasopoulos et al., 2019). In practice, this means that 3DXRD provides a view on the discrete granular mechanics for assemblies of a few hundreds of grains, whilst ND allows the study of larger, more representative sized specimens and gives a continuum view of underlying granular behaviour. This thesis focusses on the development of the ND method for granular mechanics, towards enabling better understanding of the (local) stress-strain response of granular (geo-)materials during loading, localised deformation and failure.

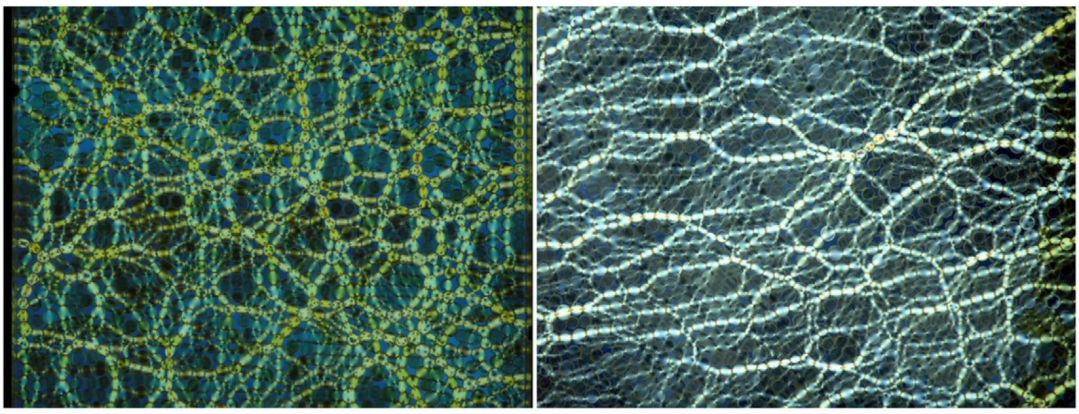

Figure 1.2: Contrasting photoelastic images of an isotropically compressed quasi-2D system of photoelastic disks (left) and a shear jammed system of the same photoelastic disks (right) (Behringer et al., 2014).

1.3 Scope and structure of this thesis

In the following chapter, fundamental concepts regarding neutron science are first outlined, followed by a presentation of the basic principles of ND and its application to study stress and strain in materials, with a particular focus on the study of granular media and their mechanics. Subsequently, Chapter 3 discusses the suggested experimental approach and the apparatuses that were developed for the purposes of this study. Furthermore, the experiments that have been conducted are outlined and an overview of representative results is also provided, whilst details on both the experimental methodologies and results are given in the appended papers. In the final chapter, the key conclusions from the work realised within the framework of this PhD project are summarised, leading to a discussion on the perspectives opened for future research.

Chapter 2

Principles of neutron diffraction measurements

> I am afraid neutrons will not be of any use to any one.[1]
>
> Sir James Chadwick

In 1920, in his Bakerian prize[2] lecture entitled *Nuclear Constitution of Atoms*, Ernest Rutherford suggested the presence of an uncharged particle (i.e., electrically neutral) in the nucleus of atoms, the neutron, that could explain the difference between the atomic mass and the atomic number (Rutherford, 1920). The existence of Rutherford's neutron was eventually proven by James Chadwick in 1932, by analysing the radiation emitted by beryllium when bombarded with α particles (Chadwick, 1932). Despite what Chadwick initially thought about neutrons (see epigraph), his discovery soon proved to be of crucial importance in nuclear and particle physics and, due to some of neutrons' unique properties, it has lead to significant advances and discoveries in a wide range of research disciplines.

The diffraction of neutrons was first demonstrated in the mid 1930s (von Halban and Preiswerk, 1936; Mitchell and Powers, 1936). However, at that time, due to the low intensity of the early neutron sources, it seemed unlikely for ND to develop into a useful experimental tool. It was not until the discovery of nuclear fission by Hahn, Meitner, and Strassmann (Hahn and Strassmann, 1939; Meitner and Frisch, 1939) and the subsequent development of nuclear reactors, that this limitation was overcome. The first, systematic ND experiments, worthy of mentioning given their significance towards the exploitation of ND, were carried out at the Oak Ridge National Laboratory, USA, mainly in the years immediately after the end of World War II (Wilkinson, 1986; Shull, 1995, and references therein), but also during the war, as part of the Manhattan Project (Mason et al., 2013,

[1] From an interview of Sir James Chadwick at the *New York Times* on February 29, 1932, shortly after his discovery of the neutron.

[2] The Bakerian Medal of the Royal Society, established in 1775, recognises exceptional and outstanding science.

and references therein). Since these early years, ND has been established as a powerful structural probe of matter and is particularly used for the study of polycrystalline materials (i.e., solid assemblies of crystals), such as metals.

In the present chapter, the principal characteristics and properties of neutrons are first outlined, together with a short overview of the kinds of sources that are currently used to generate neutrons for scientific purposes. Subsequently, the fundamental concepts of the ND methods and instrumentation for the main experimental technique used in this PhD project, neutron strain scanning (NSS), are briefly described. The chapter concludes with a discussion on the application of ND and NSS measurements to study granular media.

2.1 Neutrons: Properties and generation

Neutrons, as all quantum objects, behave both as waves and as particles (de Broglie, 1924). A fundamental concept of quantum objects' wave-particle duality is that their two natures can not be identified simultaneously. For instance, the ND phenomenon can be described by Bragg's law (see subsection 2.2.1), which considers neutrons as waves, but when it comes to the detection of neutrons after they have interacted with matter, they need to be treated as particles (Willis and Carlile, 2009; for a thorough review on the wave particle duality of neutrons, see Utsuro and Ignatovich, 2010).

As far as the wave nature of neutrons is concerned, they have a velocity-dependent de Broglie wavelength, λ, which can be calculated by,

$$\lambda = \frac{h}{m_{\mathrm{n}} v_{\mathrm{n}}}, \tag{2.1}$$

where h is Planck's constant, m_{n} is the neutron mass and v_{n} its velocity. The wavelength of neutrons with energy corresponding to room temperature (i.e., thermal neutrons) is of the same order of magnitude as the interplanar spacing (i.e., the d-spacing) of most crystals; that is, about 0.2 nm (Table 2.1), which constitutes one of the main reasons for neutrons being such a powerful probe of matter.

Neutrons are sub-atomic particles that have the unique characteristic of possessing both a spin (i.e., another form of angular momentum) and a magnetic moment (of opposite direction), despite the fact that they are uncharged[3] (Table 2.1). This combination of properties defines the behaviour of neutrons and their interaction with matter, which can be separated into two principal modes (Harroun et al., 2006). Firstly, due to their charge neutrality, the interaction with matter is weak, as they have no potential barrier to overcome (i.e., the Coulomb field surrounding the nucleus of an atom) and, therefore, the interaction is only nuclear and magnetic. Consequently, neutrons can penetrate deep

[3]In principle, for particles to have an intrinsic magnetic moment, they must possess both a spin and an electric charge. Neutron's magnetic moment is explained by the fact that it consists of three charged quarks (i.e., two down quarks, each with a charge of $-1/3$ of an electrostatic unit, and one up quark, with a charge of $2/3$ of an electrostatic unit), the magnetic moment and orbit of which is combined to give rise to the magnetic moment of a neutron.

Table 2.1: Basic properties of neutrons (Willis and Carlile, 2009).

Parameter	Value
Lifetime, τ	886 ± 1 s
Mass, m_{n}	1.67495×10^{-27} kg
Wavelength, λ	1.798 Å (for velocity of 2200 m/s)
Energy, E	25.3 meV (for velocity of 2200 m/s)
Spin, S	1/2
Magnetic moment, μ_{n}	$-1.913043(1)$ nuclear magnetons

into matter and interact with atomic nuclei through nuclear forces, plus complex nuclear interactions between the nuclear spins and magnetic moments. This first mode of neutron interaction is independent of an element's atomic number, as opposed to the interaction of X-rays. Additionally, this interaction mode explains the sensitivity of neutrons to light atoms, such as hydrogen, and their high penetrability through dense metals, as well as their different interaction with different isotopes of the same element (e.g., hydrogen and deuterium). As for the second mode of interaction, this is related to the interaction between the magnetic moment of neutrons and the magnetic moments of unpaired electrons in magnetic atoms, but this type of interaction is outside the scope of this thesis and will not be discussed any further.

The production of neutrons for scientific purposes can be achieved, primarily, with two kinds of sources, (i) steady-state nuclear reactors and (ii) accelerator based sources (see Arai and Crawford, 2009, and references therein for more information about the available neutron sources). Regarding the former, a fission chain reaction of uranium-235 atoms is generally used to produce a continuous, stable flux of neutron radiation. As to the latter, neutrons are generated by the spallation process, which involves the bombardment of a heavy metal target (e.g., mercury or tungsten) by high energy protons, which results in neutrons being released from the nuclei of the target's atoms. Although continuous spallation sources exist and are exploited much like reactor sources, the majority of spallation sources generate pulses of neutrons. Due to the fundamentally very different operating principles of the two source types, it is practically impossible to favour one over the other, since each of them has its own benefits, offering different instrument layouts and experimental methods (an elaborate discussion on this topic can be found in Willis and Carlile, 2009). For instance, reactors provide a high time-averaged intensity, whilst spallation sources offer a high peak flux. Eventually, the answer to the question of which source should be used is case-dependent, as it comes down to which instrument and employed method fits better to the objectives of an experiment.

2.2 Fundamentals of neutron diffraction

ND is, predominantly, an elastic scattering phenomenon; that is, a quantum mechanical process without any exchange of energy between the nuclei of a material's atoms and the neutron radiation (for a comprehensive review on the different neutron scattering phenomena see Pynn, 2009, whilst more complete information on the topic can be found in various readings, such as Squires, 1978, and Sivia, 2011). In general, scattering can either be coherent, when neutrons diffracted by different nuclei interfere constructively with each other, or, otherwise, incoherent. The coherent part of elastic scattering and, hence, ND can provide information on the internal crystalline structure and texture of materials, as well as the variation of these features due to external factors, such as temperature or pressure alterations.

In accordance with the fact that there are two types of neutron sources, there exist two ND measurement methods. For the case of reactor sources, the polychromatic neutron beam is, in general, monochromated and, as a result, single wavelength (SW) ND measurements are conducted with respect to a varying diffraction angle. At pulsed spallation sources, the nature of the neutron beam (i.e., pulsed and polychromatic) allows the direct recording of the time-of-flight (TOF) of neutrons, from the source to a detector, across a wide energy – or wavelength – range. Consequently, this source type offers the possibility to employ the TOF-ND method that directly provides wavelength-resolved diffraction measurements. It is noted that, in theory, TOF-ND measurements can take place at reactor sources as well, but this is less common. Below, the differences between two types of ND methods (i.e., SW-ND and TOF-ND) are discussed (subsection 2.2.1), along with the implications of those differences in the design of the two, respective, types of neutron diffractometers (subsection 2.2.3).

2.2.1 Bragg's law and basic formalism

Crystals are composed of repeating "unit cells", forming a lattice. Within a crystal, a set of lattice planes with the same orientation and spacing (i.e., a "family" of crystallographic planes), or the direction normal to them, may be labelled by the, so called, Miller indices, hkl. When neutron radiation interacts with a crystal, neutrons may be diffracted (i.e., scattered elastically) from the crystal's lattice system. In certain directions (Figure 2.1), defined by scattering angles θ^{hkl}, neutrons diffracted by adjacent planes of the corresponding $\{hkl\}$ families will remain in phase and interfere constructively with each other. The condition for constructive interference to occur can be described through Bragg's law (Bragg, 1913[4]), a relationship between the scattering angle, the d-spacing of an $\{hkl\}$ family of crystallographic planes, d^{hkl}, and the neutron wavelength,

[4]The derivation of the reflection condition by Sir William Lawrence Bragg was first presented at a meeting of the Cambridge Philosophical Society on November 11, 1912 by Sir Joseph John Thomson, but Bragg's paper was not published until February 1913.

$$n\lambda = 2d^{hkl} \sin\theta^{hkl}, \tag{2.2}$$

where n is a positive integer, expressing that the path length difference of the diffracted neutrons must be a multiple of the wavelength. The fulfillment of Bragg's law results in a maximum of scattered intensity (i.e., a reflection or Bragg peak) in a recorded diffraction pattern, which is associated with a specific hkl orientation.

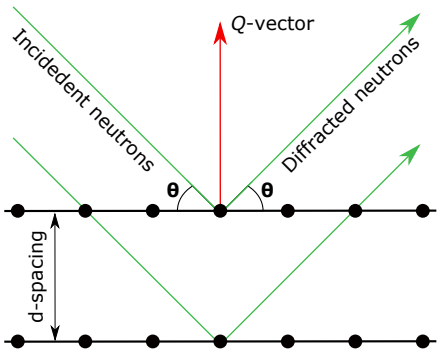

Figure 2.1: Schematic representation of Bragg's law.

For polycrystalline materials and granular media (as in this thesis), both SW-ND and TOF-ND measurements are generally realised by defining a sub-volume of a specimen that is illuminated by neutrons (i.e., the gauge volume – GV). This GV, typically of the order of a few mm^3, is determined by the intersection of the collimated incident and diffracted neutrons (see subsection 2.2.3 – Figures 2.2 and 2.3). Depending on the GV dimensions and the size of its constituent crystals, a GV may contain hundreds, or even thousands of crystals. All crystals having the same hkl orientation that fulfils Bragg's law, will belong to the respective hkl subset of scattering crystals. For SW-ND, given the fact that the incident beam is monochromatic, usually a single, or just a few (e.g., at most three to four) hkl subsets can be studied simultaneously. In the case of TOF-ND, though, the reflection condition described by Bragg's law can be satisfied for multiple (i.e., tens of) wavelengths and hkl orientations, separated in time. The diffracted neutrons, from all the partaking hkl subsets of scattering crystals, are detected at a fixed angle, 2θ, as a function of their TOF, t^{hkl}, and their wavelength is defined by making use of equation (2.1),

$$\lambda = \frac{t^{hkl} h}{m_{\mathrm{n}} L}, \tag{2.3}$$

where the velocity of the neutron has been replaced by its TOF and the length of its flight path, L.

Assuming crystal purity and defect absence, under standard experimental conditions (i.e., at room temperature and pressure), Bragg peak positions are unique in a material's characteristic diffraction pattern. Peak positions, together with width and intensity, as well as any, for instance, deformation-induced fluctuations of these parameters, provide a gateway to the study of a material's behaviour and properties down to the nanoscale

level. In particular, peak position shifts are directly related to elastic changes in d-spacing (i.e., elastic crystallographic – or grain – strains) of the respective $\{hkl\}$ family of crystallographic planes, whilst peak intensities can provide information on the distribution of crystallographic orientations (i.e., the crystalline texture) in a polycrystalline material or a granular medium (these two topics are discussed further in the present chapter). Regarding peak width variations, these are often associated with the existence of defects and sub-crystal plastic deformations (i.e., intragranular strains), such as dislocations (i.e., linear defects), but in the present work only peak position shifts are considered, to study the elastic crystallographic strains.

2.2.2 The neutron strain scanning technique

NSS is a ND technique for mapping strain and, consequently, stress deep inside polycrystalline materials and, in this work, granular media. The technique was developed in the early 1970s (first review articles were by Webster, 1991, and Hutchings, 1992) at the Harwell Laboratory, UK, and has since become a powerful non-destructive testing tool. A synopsis of NSS is given below, whilst a thorough description of the technique can be found in Hutchings et al. (2005).

Crystallographic strain measurements by ND, in general, rely on the fact that d-spacing may serve as an intrinsic strain gauge embedded in a crystal. For polycrystalline materials and granular media, there will exist at least one (i.e., for SW-ND), or multiple (i.e., for TOF-ND) hkl subsets of scattering crystals that fulfil Bragg's law within a GV illuminated by neutrons. With the application of a load, each one of these hkl subsets provides a local strain gauge, through the d-spacing variations of the constituent scattering crystals in the GV. Hence, a mean, elastic, hkl-associated micro-strain, ε^{hkl}, can be calculated for each of the subsets by,

$$\varepsilon^{hkl} = \frac{d^{hkl} - d^{hkl}_{\mathrm{ref}}}{d^{hkl}_{\mathrm{ref}}} = \frac{t^{hkl} - t^{hkl}_{\mathrm{ref}}}{t^{hkl}_{\mathrm{ref}}}, \tag{2.4}$$

where d^{hkl}_{ref} and t^{hkl}_{ref} are reference, stress-free values and it should be noted that the second part of this equation, associated to TOF, can, evidently, only be used for the TOF-ND method. The orientation of all the hkl-associated micro-strains is the same, as it is defined by the scattering Q-vector that bisects the incident and the diffracted neutron beams (Figure 2.1; see also subsection 2.2.3 – Figures 2.2 and 2.3)).

Moving a specimen in two, or three orthogonal directions, whilst keeping the GV fixed in space, provides a 2D, or 3D grid of ND measurements, respectively, thus allowing a spatially-resolved characterisation of the crystallographic strains within the specimen. As the measured crystallographic strains are purely elastic, regardless of any crystal or macroscopic plasticity in the specimen, mean, hkl-associated micro-stresses, σ^{hkl}, can be computed for each illuminated hkl subset, through Hooke's law and elastic constants that depend on the crystal system in which a material belongs (the Young's and shear moduli formulas for all seven crystal systems can be found, for instance, in Sirotin and Shaskolskaya, 1982). Once all the hkl-associated micro-stresses are calculated, it is possible to

determine the total micro-stress, σ_{micro}, of a GV. It is noted that strain and stress are second rank tensors with up to six independent components. Hence, the appropriate number of ND measurements in non-coplanar directions are necessary for them to be fully defined for a specific GV. For instance, for plane-strain loading conditions the necessary ND measurements in different directions are reduced to three, in the plane. However, due to constraints of available diffractometers, the present work involves measurements only in a single direction and, therefore, all the presented relationships are treated accordingly.

2.2.3 Neutron diffractometers

As mentioned above, there are two main kinds of neutron diffractometers, SW-ND and TOF-ND, both of which make use of the same, fundamental principle of the reflection condition described by Bragg's law.

In reactor and continuous spallation sources, diffractometers are angular dispersive (Figure 2.2), such as SALSA, the diffractometer of the ILL nuclear reactor source in France (Pirling et al., 2006). In this case, the continuous, polychromatic neutron beam is first monochromated to a chosen wavelength. After a certain neutron wavelength is obtained, the incident, monochromatic beam goes through beam defining optics, to be accurately aligned and delineated, before reaching the specimen. Similarly, the diffracted neutrons are collimated by another optics system, which is located between the specimen and the detector(s). In most cases, the angle between the incident and the diffracted beams, 2θ, is set to be as close to 90° as possible, by adjusting the position of the detector, so that the GV has a nearly square horizontal cross-section. With angular dispersive diffractometers, ND measurements are, usually, realised in a single direction, Q, and the scattered intensity is acquired as a function of the scattering angle. It is noted that if the diffractometer possesses more than one detectors, then ND measurements can be realised in multiple directions, simultaneously. As for the angular range of a detector, usually it is so narrow that, for the monochromatic beam, no more than three to four Bragg peaks can be recorded (often, just one).

Pulsed spallation source diffractometers are, generally, energy dispersive and, in this case, they are known as TOF diffractometers (Figure 2.3). A characteristic example is ENGIN-X, the diffractometer of the ISIS spallation source in the UK (Santisteban et al., 2006). As with reactor source diffractometers, a system of appropriate optics defines the neutron beam, which in this case is polychromatic, before reaching the specimen. Subsequently, diffracted neutrons are recorded by detectors usually positioned at fixed angles, which accommodate beam defining optics of their own. Most TOF diffractometers have two detectors, which are positioned at about ± 90° with respect to the incident beam and, as a result, the illuminated GV has a square cross-section in the horizontal plane. With this kind of diffractometer, ND measurements can be performed simultaneously in two directions, Q_1 and Q_2, and the scattered intensity is acquired as a function of the TOF of the detected neutrons.

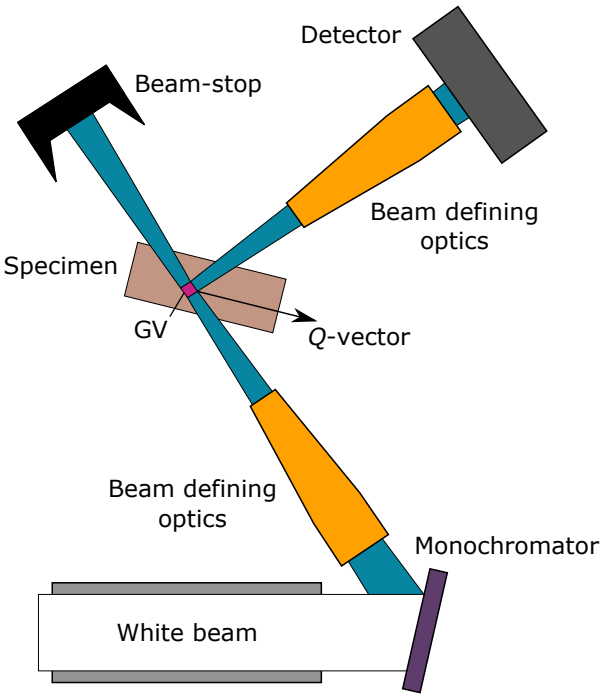

Figure 2.2: Schematic illustration of a typical angular dispersive diffractometer.

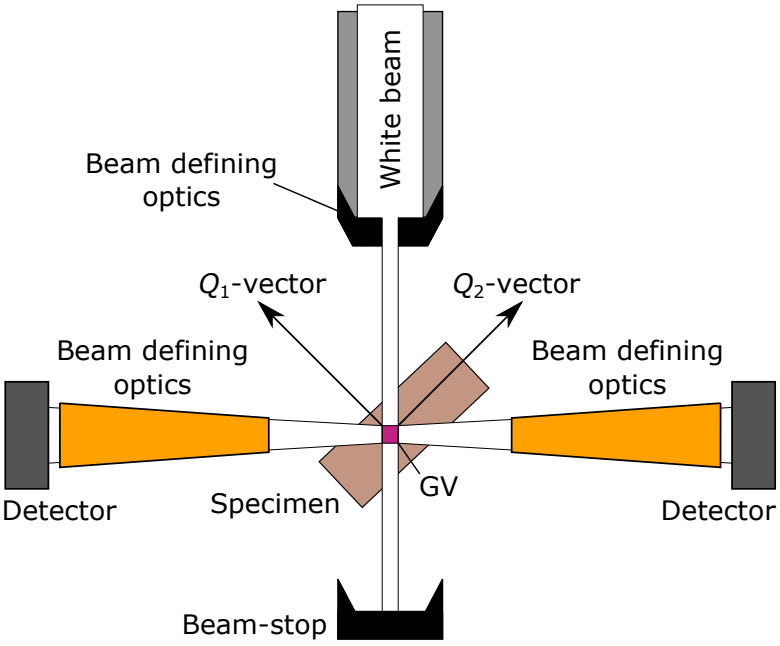

Figure 2.3: Schematic illustration of a typical energy dispersive diffractometer.

2.3 Neutron diffraction for granular media

Although one could argue that granular media are actually polycrystalline materials, they behave very differently from materials such as metals, mainly due to their particulate nature (i.e., part of the volume of a granular assembly is void) and microstructural inter-particle interactions. Nevertheless, the application of ND to study granular media is similar to that for polycrystalline materials, apart from certain aspects pointed out below, which require special attention.

For granular media the choice of the GV dimensions is central to the validity of the ND measurements, since this sub-volume of the specimen must be representative of the overall microstructure of the granular medium, in the sense that it must contain substantially populated subsets of grains in all possible *hkl* orientations. Whilst ND has been used to study granular media (see Chapter 1), there has not been much discussion of this aspect. This constitutes one of the reasons why appropriate, reference measurements are needed for granular media, which, as of yet, do not exist. A first dataset of such measurements for the material used in the current work (i.e., Fontainebleau quartz sand) is presented in this thesis (see Paper D). It is noted that, in practice, the choice of the GV dimensions also involves taking into account certain other parameters, such as the objectives of the conducted experiment, the ND instrument characteristics, the available beamtime[5] and the desired quality of the acquired data.

As far as the computation of the total micro-stress of a GV from all the inferred *hkl*-associated micro-stresses is concerned, two additional aspects need to be taken into consideration: (i) the porosity of the granular medium, as well as its variation throughout the loading, and (ii) the grain kinematics and damage. Regarding the former, the *hkl*-associated micro-strains calculated from the ND measurements are representative only of the bulk of the grains in a GV, as opposed to the granular continuum strain, which takes into consideration both the bulk of the grains and the void in between them. Therefore, to derive the bulk stress of a GV from the *hkl*-associated micro-strains, a correction needs to be applied, to exclude the voids from the computations, which can be realised by accounting for the initial porosity and its evolution throughout the loading. If this can not be determined for a specific GV, an assumption has to be adopted for it, such as utilising the total bulk ratio of the complete specimen to scale down the ND-inferred stresses (e.g., Wensrich et al.,, 2013). Furthermore, throughout the loading, grain translations, rotations and breakage will take place and so, the grains satisfying Bragg's law will not remain the same for any of the *hkl* subsets. Therefore, grain kinematics and damage, which can be considered as, or related to, texture (i.e., preferential alignment of the grains) evolution, need to be taken into account. Within a GV, the texture can be characterised by the relative Bragg peak intensity variations with respect to some reference. Consequently, the total micro-stress, σ_{micro}, of a GV at a certain load level, i, can be expressed as,

[5]At large-scale facilities, such as reactor and spallation sources, the access to an instrument is allocated to users who have applied for it, according to an experimental proposal evaluation procedure. The time period provided to a user for the realisation of an experiment is usually termed as "available beamtime".

$$\sigma_{\mathrm{micro}}(i) = \frac{V_{\mathrm{b}}}{V(i)} \sum_{hkl} \frac{w^{hkl}(i)}{\sum_{hkl} w^{hkl}(i)} E^{hkl} \varepsilon^{hkl}(i), \tag{2.5}$$

where V_{b} and V are the bulk and the total volume of the specimen, respectively, and their ratio expresses the porosity correction that needs to be accounted for throughout the loading, E^{hkl} are the hkl-associated Young's moduli and w^{hkl} are physically realistic hkl-associated weighting factors, expressing the texture evolution with respect to a reference dataset of measurements (see also Paper D), given by,

$$w^{hkl}(i) = \frac{I^{hkl}(i)/I^{hkl}_{\mathrm{ref}}}{\sum_{hkl} I^{hkl}(i)/I^{hkl}_{\mathrm{ref}}} \frac{m^{hkl}}{\sum_{hkl} m^{hkl}}, \tag{2.6}$$

where m^{hkl} is the multiplicity (i.e., the number of equivalent reflections due to crystal symmetry, the peaks of which are superimposed in a recorded diffraction pattern) and I^{hkl} and I^{hkl}_{ref} are the measured and reference intensities (i.e., the Bragg peak heights), respectively, of the respective hkl subsets of scattering grains in a GV.

2.4 Chapter summary

In the present chapter, the basic principles of the ND method and its application for the study of granular media and their mechanics have been discussed, laying the appropriate theoretical foundation for the development of the novel suggested experimental approach and the data analysis from the experiments in which it has been employed, presented in the following chapter.

Chapter 3

Experiments on quartz sand

> An experiment is a question
> which science poses to nature,
> and a measurement is the
> recording of nature's answer.
>
> Max Karl Ernst Ludwig Planck

Although the particulate nature of granular media has long been acknowledged (e.g., Terzaghi, 1920) and concepts such as strain localisation and force chains, which have been studied for almost half a century (see Chapter 1), are now considered fundamental of the behavioural analysis of granular media under load, it is still very common for them to be treated as continua. The reason for this, is that many aspects of the bulk response of granular media to load are sufficiently well described by continuum models, even if, in reality, the kinematics and deformation of individual grains is very different from how material points at the same positions act in a continuum.

Terzaghi, being ahead of his time, already reflected upon the particulate nature of granular (geo-)materials back in 1920: *"...Coulomb... purposely ignored the fact that sand consists of individual grains, and ... dealt with the sand as if it were a homogeneous mass with certain mechanical properties. Coulomb's idea proved very useful as a working hypothesis ... but it developed into an obstacle against further progress as soon as its hypothetical character came to be forgotten by Coulomb's successors. The way out of the difficulty lies in dropping the old fundamental principles and starting again from the elementary fact that sand consists of individual grains."* (Terzaghi, 1920; see also references therein). One could argue that the words of Terzaghi were forgotten, at least from an experimental perspective, as for decades after, the particulate nature of granular media was barely investigated. Paraphrasing Max Planck (see epigraph), researchers were perhaps not asking nature the right questions, as the process of asking a question (i.e., conducting an experiment) is always limited by the ability of the available tools to record an appropriate answer.

As described in Chapter 1, it was only relatively recently that the scientific community gained access to experimental tools that permit the recording of nature's answers to ques-

tions related to the mechanics of the "microworld" that lies hidden within granular media. The general objective of the experimental studies herein is to develop and exploit new tools, to improve the understanding of the (micro-)mechanisms acting within granular media that lead to degradation and, ultimately, failure during mechanical loading. Such new understanding will enable more sophisticated material models for better numerical simulations to be derived. More specifically, an advanced, multiscale experimental approach to characterise quantitatively the (micro-)structural evolution of granular (geo-)materials during loading has been developed, using Fontainebleau quartz sand as the studied material. The suggested approach associates traditional macroscale boundary measurements with mesoscale DIC-derived strain fields and NSS-inferred microscale stress distributions.

In this chapter, a brief overview of the experimental apparatuses designed for the purposes of this study is provided first. This is followed by a short presentation of the DIC technique that was used in complement to the ND measurements. The chapter continues with an outline of the experiments conducted in the study, a brief discussion on the employed ND data processing procedures and, finally, some representative results from the conducted experiments.

3.1 Experimental apparatuses

Within the framework of this PhD project, two experimental apparatuses have been designed. The main apparatus, presented first below, involves the plane-strain loading of prismatic specimens and has been developed for the realisation of the experiments involving the multiscale analysis of granular (geo-)materials by combined ND and DIC. Herein, a summary of its most important details is given, whilst a thorough presentation of its conceptual specifications and technical details can be found in Paper C. A second apparatus, which is presented subsequently, has been developed for constrained uniaxial (i.e., oedometric) loading and ND measurements.

At this point, it should be noted that the suggested approach in its original concept also involved ultrasonic measurements, to enable the association of the evolution of stresses and strains to that of the elastic properties of the material. However, due to the complexity in combining such measurements within a single experiment (to be discussed in future publications), the development has been step-wise. As a first step, the realisation of combined ND and ultrasonic experiments has already been taken, with the second apparatus presented herein that involves the oedometric loading of cylindrical specimens.

3.1.1 Plane-strain apparatus

In the work of Hall et al. (2011), it was shown that the ND method can be used to provide microscale insight into the evolution of strain in quartz sand under load, by measuring the mean, elastic crystallographic strains over a small volume of a cylindrical specimen. For that study, a simple, custom-made oedometric apparatus was employed and ND measurements were realised on a single GV, in the middle of the specimen. The current work

extends the approach of Hall et al., to gain further knowledge on how stresses are transmitted during loading and how they evolve, both spatially and temporally, throughout the material with (localised) deformation, using spatially-resolved NSS measurements during loading. However, performing NSS over multiple GVs with significant specimen coverage and sufficient spatio-temporal resolution is not a trivial endeavour, as NSS measurements require, in principle, a considerable amount of time.

For cylindrical specimens, as in the work of Hall et al., this impracticality of long measurement times could be overcome by scanning a single plane spanning the loading axis of the specimen and assuming axial symmetry (e.g., Wensrich et al., 2012; Zhang et al., 2016). In fact, Hall et al. also realised such measurements, over a 2D grid of GVs (unpublished). However, an important drawback of this approach is that features that develop in a 3D manner within the specimen can not be identified. Given the highly inhomogeneous behaviour of granular media under load (e.g., localised deformation, such as shear bands), which is known to be the rule, rather than the exception, this is a significant drawback, rendering the measurements to be, at best, ambiguous. This challenge leads to the conceptual cornerstone of the loading apparatus designed specially for the purposes of this study, which is to work with prismatic specimens in 2D, under plane-strain conditions. In plane-strain loading conditions the grain kinematics still take place, to some extent, in 3D, but the expected macroscopic localised phenomena, such as shear bands, are forced to develop in 2D.

A general view of the plane-strain apparatus developed for the main part of this study's experimental campaign is given in Figure 3.1. Paper C contains a complete description of the technical details, including technical drawings, and the various constraints that had to be met, which indicated the unsuitability of existing apparatus designs and led to the design of the presented plane-strain apparatus. In addition, some of the modifications that have already been planned for future development are outlined. It should be pointed out that the first, proof-of-concept experiment of this study was realised with a simplified prototype of the apparatus presented herein and in Paper C.

The plane-strain apparatus has been designed to accommodate specimens of approximately $60\times30\times20$ mm^3 (height $\times$ width $\times$ thickness). Plane-strain conditions are fulfilled by applying a force along the longitudinal axis of the specimen (Figure 3.1 – A), by a pair of pistons (Figure 3.1 – B & C), and deformation being limited to develop in only one of the other two directions (i.e., x-axis), through the combination of a pair of deformable, pressure-controlled cushions (Figure 3.1 – D), regulated by a pressure liquid (Figure 3.1 – E & F) to apply a confining pressure, P_c, and a pair of rigid sapphire platens (Figure 3.1 – G), which prevents any deformation in the third direction, whilst allowing the acquisition of photographs for the DIC. The minimisation of friction between the sapphire platens and both the specimen and the cushions is accomplished by lubrication with grease. The apparatus enables realistic sub-surface pressure conditions to be applied on the specimen, currently up to 3 MPa. Finally, it is noted that the prototype used in the proof-of-concept experiment did not allow the application of confining pressure. In that early prototype, the pressure cushions shown in Figure 3.1 were replaced by a pair of 2 mm thick silicone membranes, embedded in aluminum blocks that had the shape of the cushions.

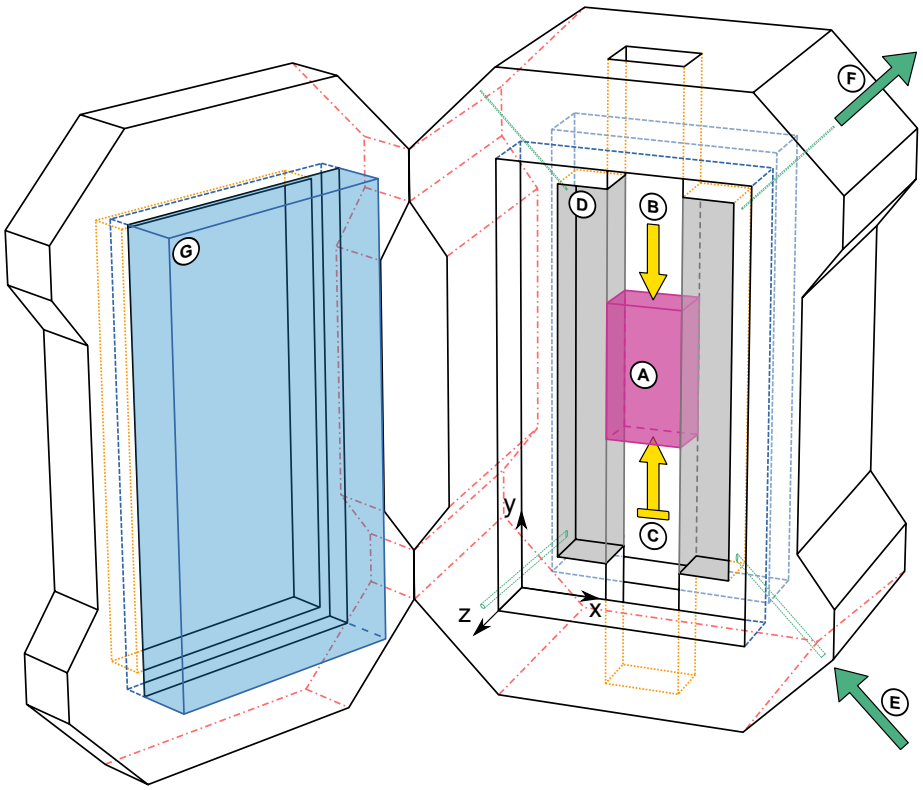

Figure 3.1: Schematic representation of the plane-strain loading apparatus. A: Specimen. B: Top piston. C: Bottom (fixed) piston. D: Pressure cushions. E: Pressure liquid supply. F: Air escape. G: Sapphire platens.

3.1.2 Oedometer

Although not in the initial objectives, a specially designed oedometer was also developed within the framework of this study. As discussed in more detail in Paper D, the realisation of oedometric experiments was decided after a series of plane-strain experiments had been conducted. The reasoning to this decision is twofold. First, as noted earlier, to make a first step towards the incorporation of ultrasonic measurements in the suggested experimental approach and second, due to the fact that certain findings from the plane-strain experiments raised questions, the answers to which were deemed to be easier to be sought under more simple loading conditions (see Paper D). A general view of the specially designed, double piston oedometric apparatus can be seen in Figure 3.2. The oedometer can accommodate specimens of 10 mm in diameter and varying height (Figure 3.2 – A), aiming for an approximate initial height of 10 mm. In Figure 3.2 it can also be seen that ultrasonic transducers can be mounted inside chambers, behind each of the pistons (Figure 3.2 – C).

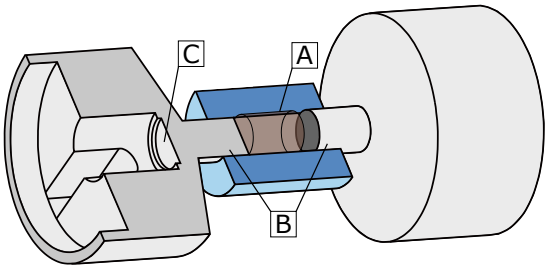

Figure 3.2: Schematic representation of the oedometric loading apparatus. A: Specimen. B: Pistons. C: Ultrasonic transducer chamber.

3.2 Digital image correlation

DIC is an optical-numerical image processing method that involves the non-contact measurement of full-field kinematics at the surface of, or within, a specimen during deformation, to derive the respective full-field strains. DIC is nowadays a quite established, standard tool in experimental mechanics and it has become increasingly popular throughout the last 30-40 years in several disciplines. Herein, a short overview of the simplest type of DIC is given, 2D DIC, which is the relevant technique for the current experiments. More complete information of the method can be found, for instance, in Sutton et al. (2009) and Hall (2012).

2D DIC is a technique that involves the utilisation of a single camera, positioned in such a way so that its image sensor is, as much as possible, parallel to the surface of the specimen being measured. As implied by its name, 2D DIC enables the measurement of 2D displacement vectors over two spatial dimensions and thus, it is applicable to planar (i.e., flat) specimens with in-plane deformation. The initially flat surface of the specimen is important to remain so, for the 2D DIC technique to be able to continuously follow the kinematics of the specimen and provide valid displacement measurements. The gradient of the 2D displacement vector field, $\boldsymbol{F}$, can be written as,

$$\boldsymbol{F} = \begin{bmatrix} 1 + \frac{\partial u}{\partial x} & \frac{\partial u}{\partial y} \\ \frac{\partial v}{\partial x} & 1 + \frac{\partial v}{\partial y} \end{bmatrix}, \tag{3.1}$$

where u and v are the displacements in the x and y directions, respectively.

DIC measurements, in general, are realised by tracking and correlating regions of the (surface) images of the specimen, acquired at different stages of deformation. Various DIC algorithms exist and the simplest methodology for a, so called, local 2D DIC analysis involves the following steps (Figure 3.3):

1. Definition of a grid of nodes (i.e., analysis points) distributed over the first (i.e., reference) image;

2. Definition of a 2D group of pixels (i.e., the correlation window, subset or motif), centred around each node of the grid;

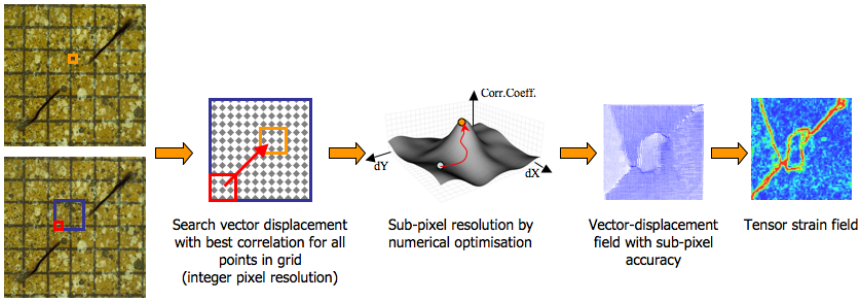

Figure 3.3: Schematic of a 2D DIC analysis approach (Hall, 2012).

3. Definition of search area (i.e., the search window) around each node of the grid in the second (i.e., deformed) image;

4. Image correlation for each node of the grid, by identifying the most similar motif in the deformed image and its position in the search area;

5. Definition of the discrete displacement (i.e., in integer numbers of pixels) for each node of the grid, as determined by the best correlation in step (4);

6. Sub-pixel refinement, given that it is rare for the displacements to be integer numbers of pixels.

Regarding the present work, the image acquisition system that was used (see following section – Figures 3.4 and 3.5) involved a high resolution (28.8 megapixel) Prosilica GT 6600 digital camera and a custom-made LED lighting system. The DIC analysis was performed using the VIC2D® software from Correlated Solutions®.

3.3 Experimental campaign

Within the framework of this study, both SW-ND and TOF-ND experiments were realised, with the SALSA and ENGIN-X neutron diffractometers, respectively. The main part of this study's experimental campaign, which involved the plane-strain loading of prismatic specimens was undertaken with both instruments (Figures 3.4 and 3.5), whilst an oedometric experiment was conducted with ENGIN-X (Figure 3.6).

The general sequence that has to be followed for the preparation and realisation of an experiment (i.e., the experimental protocol) with the plane-strain apparatus is thoroughly presented in Paper C. As for the configuration of the NSS measurements in a specimen, a schematic example is shown in Figure 3.7. At this point, it should be noted that the orientation of the simplified prototype of the plane-strain apparatus for the proof-of-concept experiment was such that ND measurements could be performed simultaneously in two directions (see also Chapter 2 – Figure 2.3 and Paper A). This is related to the absence of pressure cushions in that early prototype. As explained in detail in Paper C, the presence

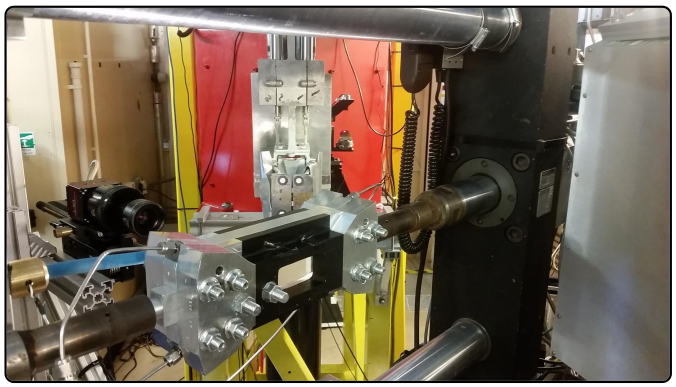

Figure 3.4: The plane-strain apparatus in the ENGIN-X neutron diffractometer at the ISIS spallation source in the UK.

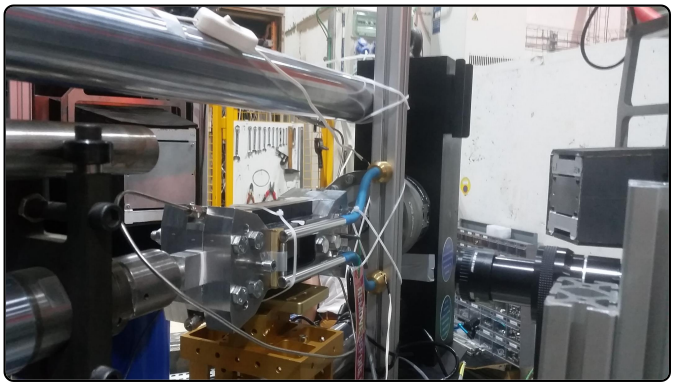

Figure 3.5: The plane-strain apparatus in the SALSA neutron diffractometer at the ILL nuclear reactor source in France.

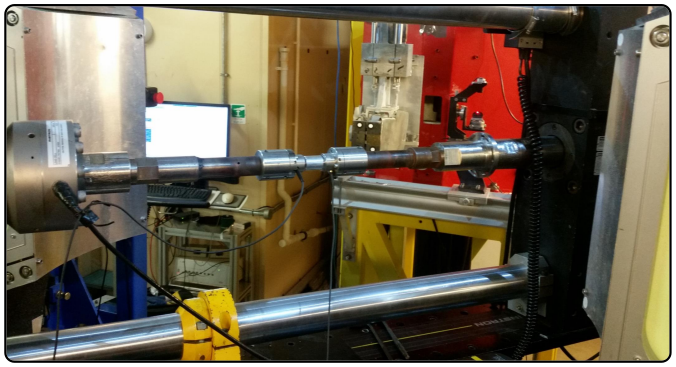

Figure 3.6: The oedometric apparatus in the ENGIN-X neutron diffractometer at the ISIS spallation source in the UK.

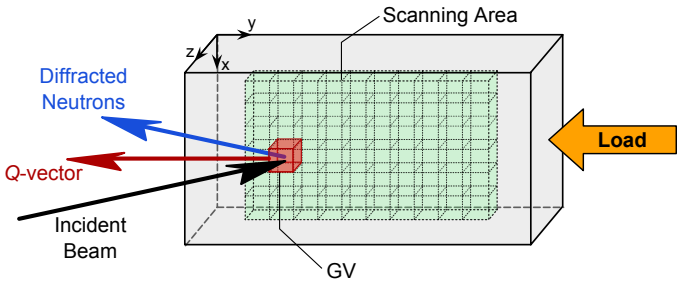

Figure 3.7: Schematic representation of the NSS measurement configuration in a prismatic specimen, for the plane-strain apparatus.

of hydrogen rich silicone rubber and pressure liquid in the flight path of neutrons makes ND measurements practically impossible and, hence, the different orientation of the actual apparatus compared to its prototype, which allows the realisation of ND measurements in a single, axial direction.

Regarding the oedometric experiment, the experimental procedure is much more straightforward and will not be discussed any further. It should only be noted that, although the presented oedometric experiment also involved the realisation of ultrasonic measurements, the data analysis is currently ongoing and, thus, is not discussed herein.

3.3.1 Conducted experiments

The material studied in all of the experiments that were realised in this study was NE34 Fontainebleau quartz sand (Table 3.1). The basic experimental details of the conducted experiments can be found in Tables 3.2 and 3.3. As far as the experiments realised under plane-strain conditions are concerned, a key aspect through the experimental campaign is the evolution in the spatial and temporal resolution of the ND measurements, as well as the spatial coverage of the specimen, as all these features have been and continue to be of foremost importance in the framework of the development of the experimental approach.

Table 3.1: Index properties of NE34 Fontainebleau quartz sand (Yang et al., 2010).

Parameter	Value
Grain shape	Sub-angular
SiO_2 purity	99.70 %
Specific gravity, G_s	2.65
Average grain size, D_{50}	210 μm
Minimum void ratio, e_{min}	0.51
Maximum void ratio, e_{max}	0.90

Table 3.2: List of conducted experiments with details regarding the loading conditions, the employed experimental methods and the status of the reporting of the results.

No. Exp.	Instrument (Facility)	Apparatus	P_c (MPa)	Experimental methods	Result reporting status
1	ENGIN-X (ISIS)	Plane-strain (prototype)	–	TOF-ND	Presented in Paper A[†]
2	SALSA (ILL)	Plane-strain	3	SW-ND	Presented in Paper A[‡]
3	ENGIN-X (ISIS)	Oedometer	–	TOF-ND Ultrasonics	Presented in Paper D
4	ENGIN-X (ISIS)	Plane-strain	3	TOF-ND DIC	Presented in Paper B[††]
5	SALSA (ILL)	Plane-strain	2	SW-ND DIC	To be presented

[†] Possible reprocessing with newly assembled reference dataset.
[‡] Reprocessing with newly assembled reference dataset underway.
[††] Reprocessing with newly assembled reference dataset in progress.

Table 3.3: List of conducted experiments with details regarding the ND measurements.

No. Exp.	Specimen coverage (%)	Grid of GVs	GV (mm^3)	Count time (min)	No. Acquisitions
1	32	5×6	$3 \times 3 \times 18$	8	13
2	12	5×10	$2 \times 2 \times 10$	13	11
3	20	–	$4 \times 4 \times 10$	3.5	153
4	56	6×10	$3 \times 3 \times 4$	4	13
5	75	$6/7 \times 12^{\dagger}$	$4 \times 4 \times 4$	3	32

[†] Mixed grid with alternating rows of 6 and 7 GVs.

3.3.2 Neutron diffraction data processing

The analysis of the ND data from the experiments using both neutron diffractometers, SALSA and ENGIN-X, can be realised with software that is provided by the respective neutron facility, ILL and ISIS. However, the processing of the majority of ND data of this study, both SW and TOF, was performed with a newly developed in-house MATLAB® code. This decision was taken due to ambiguities that were observed after processing with the provided by ISIS software the multiple peak diffraction patterns (i.e., TOF-ND data) from the proof-of-concept experiment (i.e., experiment No.1). It is noted that for the much simpler SW-ND patterns acquired with SALSA, containing significantly less Bragg peaks, it was decided, for reasons of consistency, to make use of the same MATLAB® code, appropriately modified. At this point, it should also be noted that an important difference between the SW-ND and TOF-ND methods is the fact that the Bragg peaks resulting from the former are symmetric, whilst from the latter are not. This is related to the nature of the two types of sources, which is outside the scope of this thesis and will not be discussed any further, but is taken into account in the MATLAB® code.

TOF-ND patterns are usually analysed by Rietveld refinement (Rietveld, 1969), a least squares fitting method for multiple peak profiles, which seeks an optimised crystal structure to minimise the differences between the recorded and a computed diffraction pattern. Through this method, the atomic positions and the lattice parameters of a material under study can be determined, resulting in a direct calculation of the lattice strain; that is, a strain associated to the whole unit cell, rather than individual $\{hkl\}$ families of crystallographic planes. Although Rietveld refinement has many benefits and is considered to be the standard method to analyse TOF-ND measurements, it also bears certain limitations that need to be taken into account. For instance, one significant characteristic of the conventional Rietveld refinement is that it does not account for the anisotropic response of a material, as it does not include any parameters associated with a material's elastic properties. Nevertheless, even if a material's behaviour is substantially anisotropic, Rietveld refinement will – almost always – converge to a solution (Daymond et al., 1999), which might not necessarily be representative of what the material truly experiences at the microscale. An important step towards incorporating anisotropy in Rietveld refinement was done by Daymond and coworkers (Daymond et al., 1997; 1999), who demonstrated very promising results for materials of cubic and hexagonal crystal structures under uniaxial loading. However, one of the questions they raised concerned the extendability of their approach to more complicated loading conditions than uniaxial loading. Further to that, the same group reported a failure of the method on uniaxial loading of a textured material that exhibited highly localised deformation (Daymond et al., 2000). Consequently, Daymond (2004) presented an extensive comparison of an individual peak analysis to both conventional and a more advanced Rietveld refinement, concluding that individual peak analysis was the one producing the best results and being realistic in terms of crystal physics.

For experiment No.1, the use of Rietveld refinement as a fitting method to determine directly the lattice strains throughout the granular skeleton, resulted in certain problematic features that were not possible to be overcome and led to ambiguous results. For instance,

as shown in Figure 3.8 (in blue rectangles), the fitted intensity was highly overestimated for the majority of the peaks. Whereas, there were even cases where high intensity peaks appeared in the fitted diffraction patterns, at positions that were in agreement with the theoretical diffraction pattern of quartz, which, however, should almost be non-existent according to the actual recorded data (Figure 3.8 – in green rectangles). To this end, an in-house individual peak-fitting code was developed, using the MATLAB® Curve Fitting Toolbox™ and an asymmetric Gaussian lineshape as the fitting function, adapted from Stancik and Brauns (2008),

$$G(x) = \frac{H^{hkl}\Big[1 + exp[\alpha(x - d^{hkl})]\Big]}{2} \\ exp\Bigg\{ - \frac{\Big\{(x - d^{hkl})\Big[1 + exp[\alpha(x - d^{hkl})]\Big]\Big\}^2}{8(s^{hkl})^2} \Bigg\} + B_0, \tag{3.2}$$

where the intensity of the signal (i.e., the height), H^{hkl}, the hkl-associated d-spacing value at the maximum intensity (i.e., the centroid), d^{hkl}, the width, s^{hkl}, the noise of the signal (i.e., the background), B_0, and the asymmetry factor of the lineshape, α, are the peak-fitting variables. Depending on their proximity in the recorded diffraction patterns, multiple peaks had, in some cases, to be fitted simultaneously. For these cases, the MATLAB® code and, by extension, equation (3.2) had to be adjusted in accordance with the respective number of peaks; that is, by using equation (3.2) as a sum of Gaussian lineshapes for the respective number of peaks, but with a single background value.

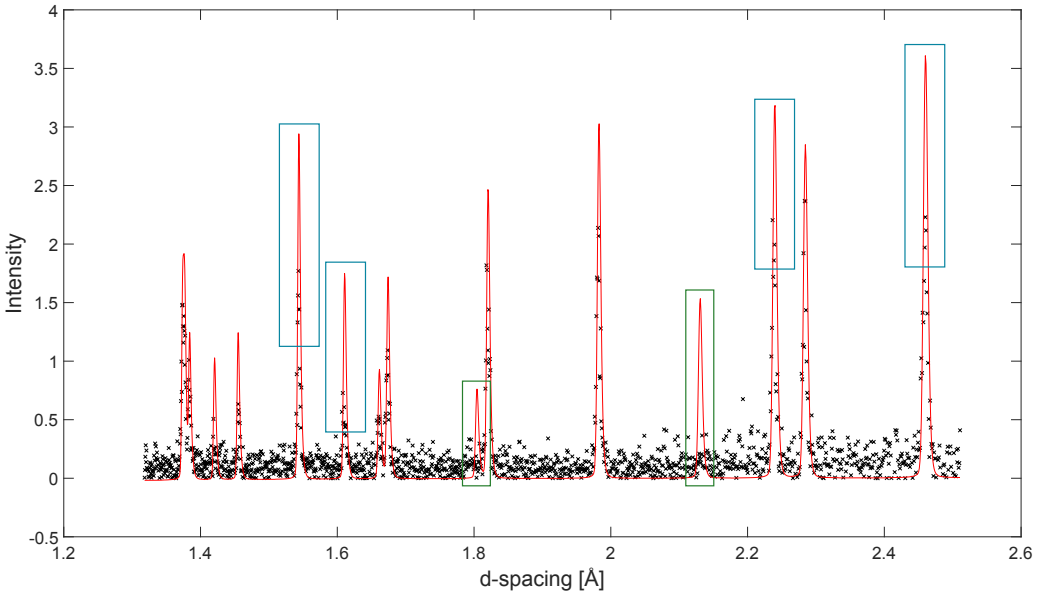

Figure 3.8: A TOF-ND pattern from the proof-of-concept experiment fitted with Rietveld refinement and examples of resulting problematic features.

The resulting, fitting-defined d^{hkl} values are then used for the computation of ε^{hkl}, through equation (2.4), whilst the fitted peak intensities, I^{hkl}, are used, for the calculation of w^{hkl}, through equation (2.6), together with respective, reference intensities that are taken from a newly assembled dataset of reference measurements for Fontainebleau quartz sand (see Paper D). Finally, these values are used in equation (2.5) to determine a realistic, in terms of crystal physics, total micro-stress. It is noted that for materials belonging to the trigonal crystal system, such as quartz, the Young's modulus in the direction normal to an $\{hkl\}$ family of crystallographic planes, E^{hkl}, which is needed for the estimation of the micro-stress through equation (2.5), can be calculated by (Sirotin and Shaskolskaya, 1982),

$$E^{hkl} = \frac{[(h^2+k^2-hk)a^2+l^2c^2]^2}{(h^2+k^2-hk)^2a^4S_{11}+hkl(h-k)3\sqrt{3}a^3cS_{14} + l^4c^4S_{33}+(h^2+k^2-hk)l^2a^2c^2(S_{44}+2S_{13})} \tag{3.3}$$

where $S_{11}, S_{13}, S_{14}, S_{33}$ and S_{44} are five out of the six independent elastic compliance coefficients characterising the materials of crystal class 32, such as quartz. At this point it should be noted that the ND data of certain experiments will be reprocessed in future work (Table 3.2), to take advantage of the newly assembled reference dataset, which had not yet been defined when they were originally processed.

3.3.3 Representative results

From all the experiments that have been conducted within the framework of this study, a selection of representative results from two experiments is given and discussed briefly herein. More specifically, selected results of experiment No.4 (i.e., a plane-strain experiment), as reported in Paper B; that is, corresponding to a single subset of scattering grains, the 211, and without performing a porosity correction, are presented first below. These are followed by the preliminary results of experiment No.3 (i.e., the oedometric experiment), as reported in Paper D, for the data analysis of which, the newly assembled reference dataset was employed, enabling multiple peaks to be accounted for in the analysis. Herein, only some basic information on this reference dataset are provided, to serve the presentation of the results from the oedometric experiment, whilst an elaborate discussion can be found in paper D.

The basic experimental details of the two presented experiments, including the loading conditions and the ND measurement specifics (i.e., the specimen coverage, the GV dimensions, etc.), are given in Tables 3.2 and 3.3. Additionally, it is noted that regarding the DIC measurements involved in experiment No.4, photographs were acquired every 5 minutes during the NSS measurements and every 6 seconds during the loading of the specimen.

Figure 3.9 shows the results from experiment No.4. In the top (Figure 3.9(b)), the DIC-derived axial component of the total strain field (left-hand side), $\varepsilon_{\mathrm{DIC,axial}}$, and the NSS-derived mappings of the axial component of the total micro-stress (right-hand side), $\sigma^{211}_{\mathrm{axial}}$, the original grid of which has been linearly interpolated onto a finer grid, are shown

for a selection of load steps. In the bottom (Figure 3.9(a)), the applied axial stress, σ_{macro}, and the mean micro-stress for each load step, $\overline{\sigma}^{211}_{\text{axial}}$, are given as functions of the macroscopic axial strain, $\varepsilon_{\text{macro}}$ (henceforth, the macro- and micro-curve, respectively).

Regarding the macro- and micro-curves, each of the three sections in which they are separated is thoroughly discussed in Paper B. In general, though, it can be stated that the two curves are in good agreement until the maximum $\overline{\sigma}^{211}_{\text{axial}}$ is reached, despite the

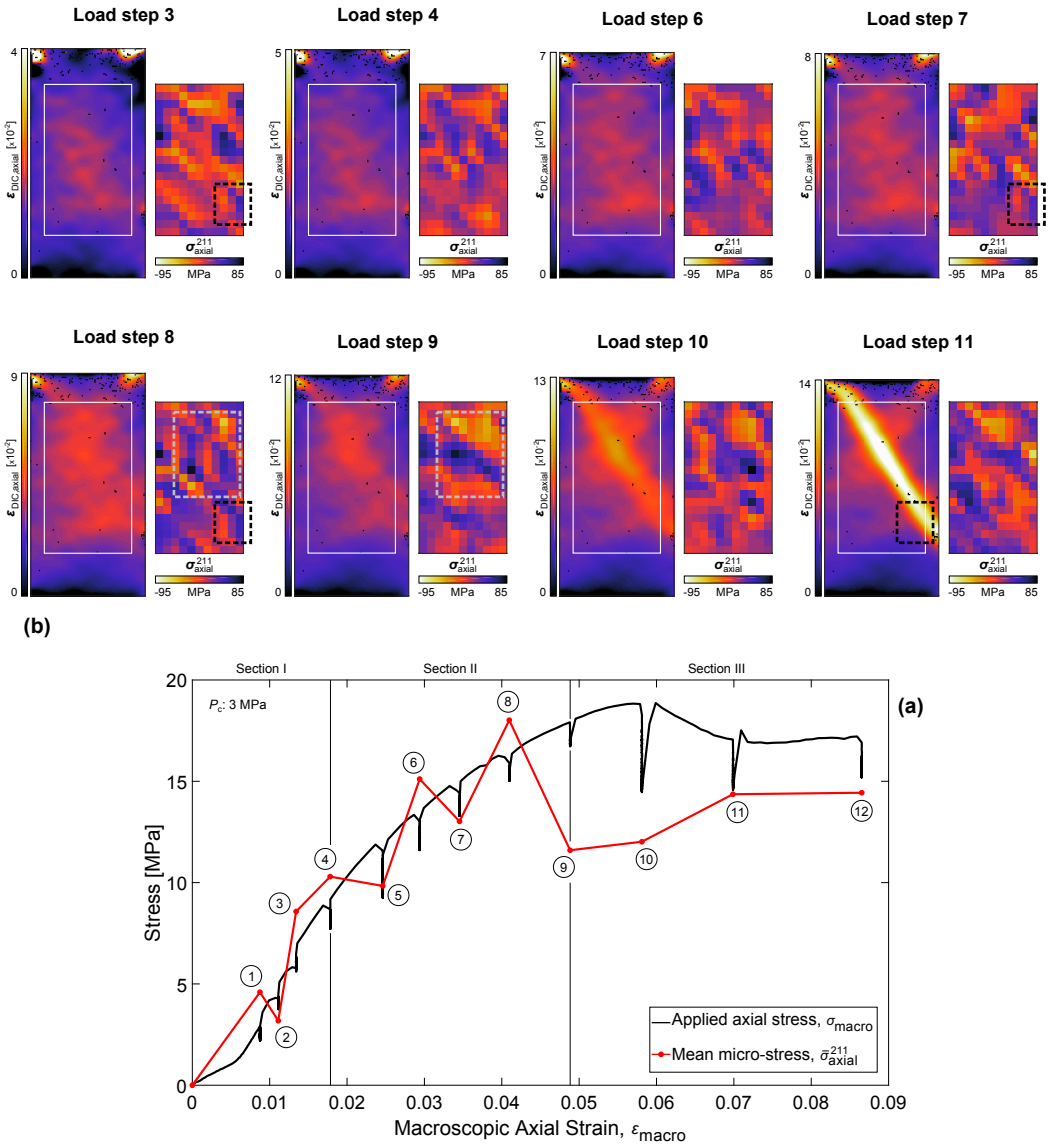

Figure 3.9: Experiment No.4 – (a): The applied axial stress (in black) and the mean axial component of the micro-stress (in red), as functions of the macroscopic axial strain. (b): The DIC-derived axial component of the total strain field (left) and the NSS-derived mappings of the axial component of the total micro-stress (right), for selected load steps.

fluctuations. The subsequent drop of the micro-curve, as well as the preceding fluctuations, can be interpreted as being related to rotation of the maximum micro-stress away from the axial direction (i.e., decreasing $\sigma^{211}_{\text{axial}}$), which might be associated with the progressive formation and, eventually, slipping of an inclined localised deformation zone.

As for the comparison of the micro-stress mappings to the DIC results, a general remark is that a relatively good and, in certain cases, prominent correlation can be made. In particular, it is worth noting the general spatial accordance of the high compression features (i.e., in darker colours) throughout the mappings, spanning from the upper-left corner to the middle and bottom of the right-hand side, to the DIC-derived strain field evolution. The development of these features implies the formation of what appears to be a shear zone, progressing into a shear band, which is consistent with the anticipated behaviour of a specimen loaded under plane-strain conditions. A characteristic example is the transition from the 8^{th} to the 9^{th} load step, where the more vertical features that evolve to more inclined features indicated by the dashed grey rectangles in Figure 3.9(b), coincide – remarkably – with the development of the regions of localised strain into a more evident diagonal structure in the corresponding DIC results. Another region of the mappings worth attention, is the one indicated by the dashed black rectangles in the 3^{rd}, 7^{th}, 8^{th} and 11^{th} load step mappings in Figure 3.9(b). As shown in the DIC results, this is the region that the shear band, eventually, slips (i.e., at the 11^{th} load step). Interestingly enough, this region appears to have experienced highly localised stresses almost from the very beginning of the loading, highlighting the need for further investigation.

However, certainly there exist features that do not correlate between the DIC and NSS results, but since through the two methods different properties are being characterised, complete structural agreement should not be expected. In fact, these differences might reveal more information on the (micro-)mechanisms that lead to macroscopic material failure, which is the focus of the, currently ongoing, reprocessing of the ND data for experiment No.4, involving multiple *hkl* subsets of grains taken into account in the calculations, based on the findings from Paper D.

Figures 3.10(a) and 3.10(b) show the results from experiment No.3, in particular, the macroscopic stress-strain response in comparison to the ND-inferred micro-stress of a specimen during oedometric monotonic loading/unloading. In Figure 3.10(a), the micro-stress has been computed using equation (2.5), whilst in Figure 3.10(b), the evolution of the porosity correction has not been accounted for (i.e., the ratio of the bulk over the total volume in equation (2.5) has been disregarded). In both figures the raw micro-stress data are presented together with a smoothed version, to enable the general trend to be better appreciated. For the latter, the Savitzky-Golay filter provided by MATLAB® has been used, a method that is suitable for rapidly varying data, such as the raw data presented in Figures 3.10(a) and 3.10(b).

The *hkl* subsets of grains chosen to be taken into consideration for the analysis of the ND data are seven out of the 10 of the reference dataset, which is presented in Table 3.4, without including the 103, the 210 and the 113. The reasoning behind this choice is given in detail in Paper D. Regarding the assessment of the curves presented in Figures 3.10(a), until about 0.6 in axial strain they seem to be in good agreement. After that point, no

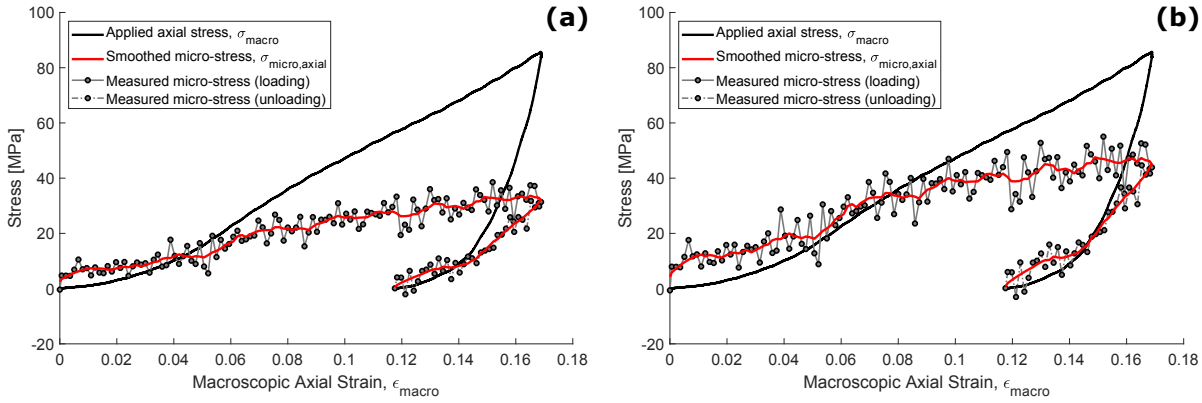

Figure 3.10: Experiment No.3 – The applied axial stress (in black), together with the axial component of the raw micro-stress (in grey) and its smoothed version (in red), which are calculated with the evolution of the porosity accounted for (a) and not accounted for (b), as functions of the macroscopic axial strain.

meticulous examination is needed to notice how different the macroscopic and microscopic responses are. As various factors may have contributed to this, a first question that is raised, simply by comparing Figures 3.10(a) and 3.10(b), is how accurate is the assumption to utilise the total, macroscopic bulk ratio in a microscale data based calculation realised for a sub-volume of the specimen, which in this case corresponds to only 20 % of its total volume. The stress drop between the two micro-stress evaluations is of the order of 30 %, which, perhaps, is too high and, in any case, leads to questioning of this assumption and highlights the need for further investigation. For instance, the fact that the specimen coverage for the ND measurements was so low might mean that the stresses simply passed around the scanned volume, but were still distributed throughout the granular skeleton. Most likely, though, a large part of the discrepancy should be attributed to load transfer from the specimen to the confining aluminum cylinder of the oedometer, as the friction between the sand grains and the aluminum walls is deemed to have reached very high levels with increasing loading.

The data analysis for experiment No.3 is ongoing and, for instance, ND measurements have also been realised on the transversal (i.e., radial) direction of the specimen, but have not yet been fully processed. Furthermore, supplementary experiments such as this one should be realised, but designed in a slightly different way, so that a bigger part, if possible all, of the specimen is monitored by ND and, hence, a more complete picture of its microscale behaviour can be analysed. Additionally, part of the confining aluminum cylinder could be measured, to investigate the load transfer to it from the granular skeleton.

Table 3.4: The 10 *hkl* subsets of grains forming the newly assembled reference dataset for Fontainebleau quartz sand, together with their d-spacing (Å), as derived by the peak-fitting analysis, and their Young's modulus (GPa), as computed by equation (3.3).

hkl subset of grains	d-spacing, d^{hkl}	Young's modulus, E^{hkl}
110	2.4588	78.25
102	2.2833	105.24
111	2.2384	101.74
201	1.9815	89.65
112	1.8195	105.24
202	1.6734	101.74
103	1.6606	104.55
210	1.6099	78.25
211	1.5430	72.87
113	1.4544	104.55

3.4 Chapter summary

In this chapter, the suggested novel multiscale experimental approach for the study of granular media and their mechanics has been presented. Furthermore, the involved developed apparatuses have been outlined, with the main focus being on the plane-strain apparatus, which has been specially designed to enable the suggested approach, combining ND and DIC measurements. In addition, the experiments realised with these apparatuses have been presented, together with the adopted ND data analysis procedure that was followed to process the acquired measurements. Key role in this procedure have both the newly developed in-house MATLAB® code and the newly assembled dataset of reference measurements for the material studied in this PhD project.

Chapter 4

Conclusions and future perspectives

> If I have seen further it is by
> standing on the shoulders of giants.
>
> Sir Isaac Newton

The objective of this study has been to provide new possibilities for better understanding of the mechanics in granular media, in particular, the (micro-)mechanisms related to material degradation leading, eventually, to material failure. The main focus has been on studying the evolution of stress distributions within a granular medium under load, a key, missing piece of information in the investigation of granular mechanics, by realising appropriate, spatially-resolved (local) measurements of both stress and strain, simultaneously. In this chapter, the key conclusions of this thesis are summarised, followed by a discussion of the perspectives opened for future research.

4.1 Conclusions

The type of granular medium studied within the framework of this PhD project is a granular geomaterial: high purity quartz sand and, more specifically, Fontainebleau quartz sand. To achieve the envisaged combined characterisation of (local) stress and strain behaviours, a novel experimental approach, based on neutron diffraction (ND) and digital image correlation (DIC), has been developed. The ND method provides information on the distribution of stresses throughout the granular skeleton of the material, by inference from measured crystallographic strains of the grains, whilst DIC provides the complementary total strain field mapping. A key component that enabled this novel approach was the development of a new plane-strain apparatus. This specially designed loading apparatus and the combined measurements it enabled, allowed a completely novel, multiscale analysis for granular (geo-)materials, by associating traditional macroscale boundary measurements with the mesoscale strain fields, derived from DIC, and the microscale stress distributions, inferred by the ND measurements.

The design of the plane-strain apparatus involved several challenging constraints, which are thoroughly discussed in Paper C, appended herein, along with its conceptual specifications and technical details. The results from the first series of combined ND and DIC experiments realised with the apparatus have demonstrated its potential, as well as that of the suggested experimental approach (see Papers A and B). The correlation of structures observed in the NSS and DIC results clearly indicates that the combination of the two methods in a single experiment can provide novel insight into the coupled evolution of stress and strain distributions throughout the material, as the deformation develops towards (localised) material failure. However, since through the two methods different properties are being characterised, these correlations are not always straightforward and require further study to comprehend structural differences between the DIC-derived strain fields and the NSS-inferred stress distributions. In fact, it is likely that non-agreeing features might reveal more information on the mechanics of granular media across different scales.

The analysis of the described plane-strain experiments highlighted the need for appropriate, ND reference measurements for granular media, which, as of yet, do not exist, but are key for the effective employment of the ND method. As a result, it was deemed necessary to take a step backwards and realise such measurements for the material under study (see Paper D), so as to set the proper foundation both for the better analysis of the experimental data acquired within the framework of the current project and for future experiments. With this, newly assembled reference dataset of ND measurements it is now possible, by a physically realistic weighting factor, to assess the orientation-dependent contribution of different subsets of grains to the definition of an average micro-stress response of the granular skeleton, which is representative of the microscopic level material behaviour during loading, avoiding the uncertainties of boundary measurements.

4.2 Future perspectives

A number of experiments has been realised within the framework of this study, using the suggested experimental approach that combines ND and DIC measurements through a novel plane-strain apparatus. Regarding the ND data, the analysis has provided some new insights into the (micro-)mechanics of granular media and has established the core of the data processing protocol, which is based on a newly developed in-house peak-fitting code and a material-specific reference dataset of ND measurements. However, there is a wealth of further information that might be gained from these experimental data, both ND and DIC, which is the focus of ongoing work. More specifically, this combination of measurements provides a gateway to the study of stress-strain relationships in a localised manner.

Key questions with the development of a new experimental approach concern the possible sources of uncertainty. In the case of the approach suggested herein, most of these are, in fact, strongly connected to the lack of appropriate ND reference and calibration measurements for granular media. This issue has been addressed (see Paper D), but requires

further attention, as the current reference dataset should be enhanced, by incorporation of new ND measurements. Additionally, this task should be undertaken for other kinds of sand and granular media, in general.

Future developments of the plane-strain apparatus should involve the utilisation of smaller specimens, a new geometry for the main body of the apparatus and the involvement of (even) more neutron efficient materials, such as the use of fluorinated silicone rubber for the manufacturing of the pressure cushions (see Paper C). By doing so, the new version of the apparatus will allow higher operation pressures, higher spatial and temporal resolution (i.e., larger, denser scanning grid and more load steps, respectively) and the realisation of ND measurements in, at least, two directions, simultaneously. In fact, the next generation neutron diffractometers, such as the one at the currently-under-construction European Spallation Source (ESS), will be able to offer the possibility for simultaneous realisation of ND measurements in more than two directions. Hence, the full analysis of the in-plane grain-strain and, thus, stress tensor should be possible.

Finally, as noted in Chapter 3, the original concept of the suggested experimental approach involved the combined realisation of ND, DIC and ultrasonic measurements, to enable the association of the evolution of stresses and strains to that of the elastic properties of the material. The first step towards accomplishing this is the realisation of combined ND and ultrasonic experiments, which has already been taken for the case of oedometric loading conditions (see Chapter 3) and their analysis is currently ongoing. As a next step, the new version of the apparatus will offer the possibility of performing simultaneous DIC and ultrasonic measurements. The third and last step, which is the most challenging, is the employment of all three methods within a single experiment. This will provide an even greater wealth of information on granular mechanics, as well as a number of new entertaining technical challenges!

Summary of appended papers

Paper A: Neutron diffraction (ND), a technique nominally used for residual stress analysis in metals, was successfully used, for the first time, to map, in a spatio-temporal manner, the intragranular strains in a quartz sand specimen under load. For the loading of the specimen, a new plane-strain apparatus, developed specially for ND experiments, was employed. In Paper A representative preliminary results were presented, aiming to highlight the potential of the ND method for the study of granular media.

Paper B: Under the effect of loading, granular (geo-)materials exhibit highly inhomogeneous behaviours and mechanics, which indicate the existence of varying and evolving local stress-strain relationships throughout the granular skeleton. To understand the (micro-) mechanisms related to such behaviours that eventually lead to material failure, a combination of simultaneous measurements by neutron diffraction (ND) and digital image correlation (DIC) was realised on a quartz sand specimen, with a modified version of the plane-strain apparatus used for the experiments presented in Paper A. The ND measurements provided information on the evolution of the stress distribution in the specimen, by inference from measured crystallographic strains of the quartz grains, whilst DIC was used to characterise the total strain field. This constitutes a novel experimental approach to study granular media and their mechanics, the first results of which revealed intricate information regarding deformation mechanisms in granular (geo-)materials and are presented in Paper B.

Paper C: A key, missing piece of information in the investigation of the (micro-)mechanisms acting during the deformation of granular media, eventually leading to their failure, is related to the evolution of force/stress distribution. In the endeavour of enriching our understanding of the highly complex (micro-)mechanics of granular media, a novel experimental approach has been developed (presented in Paper B), associating traditional boundary measurements with microscale information acquired by neutron diffraction (ND), as well as digital image correlation (DIC), at a mesoscale in between. To enable this combination of measurements, a new, specially designed plane-strain apparatus for granular (geo-)materials has been developed, employed for the first time for the experiment reported in Paper B. In Paper C the apparatus is thoroughly described and its full potential is discussed, along with possible future developments.

Paper D: Over the past few years, neutron diffraction (ND), a well established technique to investigate the stresses in bulk polycrystalline materials, such as metals, has been successfully employed to study granular media and their mechanics. After a series of experiments that has been realised (presented in Papers A and B) on quartz sand, in particular, the produced results involved many ambiguities, which gave rise to several challenging questions to be answered. These experimental developments highlighted the need for appropriate reference, material-specific ND measurements for granular media, which, until now, did not exist. To address this need, a newly assembled dataset of reference measurements for Fontainebleau quartz sand (i.e., the same material that has been studied in Papers A, B and C, as well) is presented in this paper. Such a reference dataset, enables the better analysis of ND data and, additionally, offers the opportunity for more informed decisions regarding the choice of ND measurements in future experiments.

References

Allersma, H. G. B., 1982. Determination of the stress distribution in assemblies of photoelastic particles. Experimental Mechanics 22 (9), 336–341.

Andreotti, B., Forterre, Y., Pouliquen, O., 2013. Granular media: between fluid and solid. Cambridge University Press.

Arai, M., Crawford, K., 2009. Neutron sources and facilities. In: Neutron imaging and applications. pp. 13–30.

Athanasopoulos, S. D., Hall, S. A., Kelleher, J. F., 2019. A novel multiscale neutron diffraction based experimental approach for granular media. Géotechnique Letters (Ahead of print), 1–15.

Behringer, R. P., Bi, D., Chakraborty, B., Clark, A., Dijksman, J., Ren, J., Zhang, J., 2014. Statistical properties of granular materials near jamming. Journal of Statistical Mechanics: Theory and Experiment 2014 (6), 06004.

Bragg, W. L., 1913. The Diffraction of Short Electromagnetic Waves by a Crystal. In: Proceedings of the Cambridge Philosophical Society 17. pp. 43–57.

Brujić, J., Edwards, S. F., Grinev, D. V., Hopkinson, I., Brujić, D., Makse, H. A., 2003. 3D bulk measurements of the force distribution in a compressed emulsion system. In: Faraday Discussions 123. pp. 207–220.

Chadwick, J., 1932. Possible existence of a neutron. Nature 129 (3252), 312.

Coulomb, C. A., 1776. Essai sur une application des regles de maximis et minimis quelques problemes de statique, relatits a l'architecture. In: Academie Royale de Science 7, pp. 343–382.

Darcy, H., 1856. Les fontaines publiques de la ville de Dijon. Dalmont.

Daymond, M. R., 2004. The determination of a continuum mechanics equivalent elastic strain from the analysis of multiple diffraction peaks. Journal of Applied Physics 96 (8), 4263–4272.

Daymond, M. R., Bourke, M. A. M., Von Dreele, R. B., 1999. Use of Rietveld refinement to fit a hexagonal crystal structure in the presence of elastic and plastic anisotropy. Journal of Applied Physics 85 (2), 739–747.

Daymond, M. R., Bourke, M. A. M., Von Dreele, R. B., Clausen, B., Lorentzen, T., 1997. Use of Rietveld refinement for elastic macrostrain determination and for evaluation of plastic strain history from diffraction spectra. Journal of Applied Physics 82 (4), 1554–1562.

Daymond, M. R., Tomé, C. N., Bourke, M. A. M., 2000. Measured and predicted intergranular strains in textured austenitic steel. Acta Materialia 48 (2), 553–564.

De Broglie, L., 1924. Recherches sur la théorie des quanta. Doctoral Thesis.

Desrues, J., Andò, E., Mevoli, F. A., Debove, L., Viggiani, G., 2018. How does strain localise in standard triaxial tests on sand: Revisiting the mechanism 20 years on. Mechanics Research Communications 92, 142–146.

Drescher, A., De Jong, G. D. J., 1972. Photoelastic verification of a mechanical model for the flow of a granular material. Journal of the Mechanics and Physics of Solids 20 (5), 337–340.

Faraday, M., 1831. On a peculiar class of acoustical figures; and on certain forms assumed by groups of particles upon vibrating elastic surfaces. In: Philosophical transactions of the Royal Society of London 121. pp. 299–340.

Goodman, R. E., 1999. Karl Terzaghi: The engineer as artist. American Society of Civil Engineers Press.

Hahn, O., Strassmann, F., 1939. Über den Nachweis und das Verhalten der bei der Bestrahlung des Urans mittels Neutronen entstehenden Erdalkalimetalle. Naturwissenschaften 27 (1), 11–15.

Hall, S. A., 2012. Digital image correlation in experimental geomechanics. In: ALERT Geomaterials Doctoral Summer School 2012. pp. 69–102.

Hall, S. A., Bornert, M., Desrues, J., Pannier, Y., Lenoir, N., Viggiani, G., Bésuelle, P., 2010. Discrete and continuum analysis of localised deformation in sand using X-ray [mu] CT and volumetric digital image correlation. Géotechnique 60 (5), 315.

Hall, S. A., Wright, J., 2015. Three-dimensional experimental granular mechanics. Géotechnique Letters 5 (4), 236–242.

Hall, S. A., Wright, J., Pirling, T., Andò, E., Hughes, D. J., Viggiani. G., 2011. Can intergranular force transmission be identified in sand?. Granular Matter 13 (3), 251–254.

Harroun, T. A., Wignall, G. D., Katsaras, J., 2006. Neutron scattering for biology. In: Neutron Scattering in Biology. pp. 1–18.

Hurley, R. C., Hall, S. A., Andrade, J. E., Wright, J., 2016. Quantifying interparticle forces and heterogeneity in 3D granular materials. Physical Review Letters 117 (9), 098005.

Hurley, R. C., Hall, S. A., Wright, J. P., 2017. Multi-scale mechanics of granular solids from grain-resolved X-ray measurements. In: Proceedings of the Royal Society A: Mathematical, Physical and Engineering Sciences 473 (2207). 20170491.

Hutchings, M. T., 1992. Neutron diffraction measurement of residual stress fields—the engineer's dream come true?. Neutron News 3 (3),14–19.

Hutchings, M. T., Withers, P. J., Holden, T. M., Lorentzen, T., 2005. Introduction to the characterization of residual stress by neutron diffraction. CRC Press.

Jaeger, H. M., Nagel, S. R., Behringer, R. P., 1996. Granular solids, liquids, and gases. Reviews of Modern Physics 68 (4), 1259.

Majmudar, T. S., Behringer, R. P., 2005. Contact force measurements and stress-induced anisotropy in granular materials. Nature 435 (7045), 1079.

Mason, T. E., Gawne, T. J., Nagler, S. E., Nestor, M. B., Carpenter, J.M., 2013. The early development of neutron diffraction: science in the wings of the Manhattan Project. Acta Crystallographica Section A: Foundations of Crystallography 69 (1), 37–44.

Meitner, L., Frisch, O. R., 1939. Products of the fission of the uranium nucleus. Nature 143 (3620), 471.

Mitchell, D. P., Powers, P. N., 1936. Bragg reflection of slow neutrons. Physical Review 50 (5), 486.

Muir Wood, D., Lesniewska, D., 2011. Stresses in granular materials. Granular Matter 13 (4), 395–415.

Oda, M., Takemura, T., Takahashi, M., 2004. Microstructure in shear band observed by microfocus X-ray computed tomography. Géotechnique 54 (8), 539–542.

Papadopoulos, L., Porter, M. A., Daniels, K. E., Bassett, D. S., 2018. Network analysis of particles and grains. Journal of Complex Networks 6 (4), 485–565.

Peters, J. F., Muthuswamy, M., Wibowo, J., Tordesillas, A., 2005. Characterization of force chains in granular material. Physical Review E 72 (4), 041307.

Pirling, T., Bruno, G., Withers, P. J., 2006. SALSA—A new instrument for strain imaging in engineering materials and components. Materials Science and Engineering: A 437 (1), 139–144.

Pynn, R., 2009. Neutron scattering—a non-destructive microscope for seeing inside matter. In: Neutron applications in earth, energy and environmental sciences. pp. 15–36.

Reynolds, O., 1885. On the dilatancy of media composed of rigid particles in contact. With experimental illustrations. The London, Edinburgh, and Dublin Philosophical Magazine and Journal of Science 20 (127), 469–481.

Rietveld, H., 1969. A profile refinement method for nuclear and magnetic structures. Journal of Applied Crystallography 2 (2), 65–71.

Rutherford, E., 1920. Bakerian lecture: nuclear constitution of atoms. In: Proceedings of the Royal Society of London. Series A 97 (686). pp.374–400.

Saadatfar, M., Sheppard, A. P., Senden, T. J., Kabla, A. J., 2012. Mapping forces in a 3D elastic assembly of grains. Journal of the Mechanics and Physics of Solids 60 (1), 55–66

Santamarina, J. C., 2003. Soil behavior at the microscale: particle forces. In: Soil behavior and soft ground construction. pp. 25–56.

Santisteban, J. R., Daymond, M. R., James, J. A., Edwards, L., 2006. ENGIN-X: a third-generation neutron strain scanner. Journal of Applied Crystallography 39 (6), 812–825.

Shull, C. G., 1995. Early development of neutron scattering. Reviews of Modern Physics 67 (4), 753.

Sirotin, I. Y., Shaskolskaya, M. P., 1982. Fundamentals of Crystal Physics. Mir Publishers.

Sivia, D. S., 2011. Elementary scattering theory: for X-ray and neutron users. Oxford University Press.

Squires, G. L., 1978. Introduction to the theory of thermal neutron scattering. Cambridge University Press.

Stancik, A. L., Brauns, E. B., 2008. A simple asymmetric lineshape for fitting infrared absorption spectra. Vibrational Spectroscopy 47 (1), 66–69.

Sutton, M. A., Orteu, J. J., Schreier, H., 2009. Image correlation for shape, motion and deformation measurements: basic concepts, theory and applications. Springer Science & Business Media.

Terzaghi, K., 1920. New facts about surface-friction. Physical Review 16 (1), 54.

Terzaghi, K., 1943. Theoretical Soil Mechanics. John Wiley & Sons.

Utsuro, M., Ignatovich, V. K., 2010. Handbook of neutron optics. John Wiley & Sons.

Viggiani, G., Hall, S. A., 2008. Full-field measurements, a new tool for laboratory experimental geomechanics. In: Proceedings of the 4$^{\text{th}}$ International Symposium on Deformation Characteristics of Geomaterials. pp. 3–26.

Von Halban, H., Preiswerk, P., 1936. Experimental evidence of neutron diffraction. Comptes Rendus de l Academie des Sciences 203, 73.

Webster, P. J., 1991. Neutron strain scanning. Neutron News 2 (2), 19–22.

Welland, M., 2009. Sand: the never-ending story. University of California Press.

Wensrich, C. M., Kisi, E. H., Zhang, J. F., Kirstein, O., 2012. Measurement and analysis of the stress distribution during die compaction using neutron diffraction. Granular Matter 14 (6), 671–680.

Wensrich, C. M., Kisi, E. H., Luzin, V., 2013. Non-contact stress measurement in granular materials via neutron and X-ray diffraction: theoretical foundations. Granular Matter 15 (3), 275–286.

Wilkinson, M. K., 1986. Early history of neutron scattering at oak ridge. Physica B+ C 137 (1-3), 3–16.

Willis, B. T. M., Carlile, C. J., 2009. Experimental neutron scattering. Oxford University Press.

Yang, Z. X., Jardine, R. J., Zhu, B. T., Foray, P., Tsuha, C. D. H. C., 2010. Sand grain crushing and interface shearing during displacement pile installation in sand. Géotechnique 60 (6), 469.

Zhang, J. F., Wensrich, C. M., Kisi, E. H., Luzin, V., Kirstein, O., and Smith, A. L., 2016. Stress distributions in compacted powders in convergent and stepped dies. Powder Technology 292, 23–30.

Zhou, J., Long, S., Wang, Q., Dinsmore, A. D., 2006. Measurement of forces inside a three-dimensional pile of frictionless droplets. Science 312 (5780), 1631–1633.